Regulation of CD4+NKG2D+ Th1 Cells in Patients with Metastatic Melanoma Treated with Sorafenib: Role of IL-15Rα and NKG2D Triggering

Ana I. Romero[1,7], Nathalie Chaput[1,7,8], Vichnou Poirier-Colame[1,7,8], Sylvie Rusakiewicz[1,7,8], Nicolas Jacquelot[1,7,8], Kariman Chaba[1,7], Erwan Mortier[10], Yannick Jacques[10], Sophie Caillat-Zucman[11], Caroline Flament[1,7], Anne Caignard[12], Meriem Messaoudene[12], Anne Aupérin[2], Philippe Vielh[6], Philippe Dessen[1,4], Camillo Porta[14], Christine Mateus[3,5], Maha Ayyoub[9], Danila Valmori[9], Alexander Eggermont[1], Caroline Robert[3,5], and Laurence Zitvogel[1,7,8,13]

Abstract

Beyond cancer-cell intrinsic factors, the immune status of the host has a prognostic impact on patients with cancer and influences the effects of conventional chemotherapies. Metastatic melanoma is intrinsically immunogenic, thereby facilitating the search for immune biomarkers of clinical responses to cytotoxic agents. Here, we show that a multi-tyrosine kinase inhibitor, sorafenib, upregulates interleukin (IL)-15Rα *in vitro* and *in vivo* in patients with melanoma, and in conjunction with natural killer (NK) group 2D (NKG2D) ligands, contributes to the Th1 polarization and accumulation of peripheral CD4+NKG2D+ T cells. Hence, the increase of blood CD4+NKG2D+ T cells after two cycles of sorafenib (combined with temozolomide) was associated with prolonged survival in a prospective phase I/II trial enrolling 63 patients with metastatic melanoma who did not receive vemurafenib nor immune checkpoint–blocking antibodies. In contrast, in metastatic melanoma patients treated with classical treatment modalities, this CD4+NKG2D+ subset failed to correlate with prognosis. These findings indicate that sorafenib may be used as an "adjuvant" molecule capable of inducing or restoring IL-15Rα/IL-15 in tumors expressing MHC class I–related chain A/B (MICA/B) and on circulating monocytes of responding patients, hereby contributing to the bioactivity of NKG2D+ Th1 cells. *Cancer Res; 74(1); 68–80. ©2013 AACR.*

Introduction

Therapy for metastatic melanoma remained unsatisfactory for many decades. A range of various treatment modalities based on chemotherapy has had little impact on survival (1). As a single agent, dacarbazine (DTIC) has been commonly used (2). Some investigators substitute DTIC with temozolomide (related oral alkylating agent) for its convenience of administration and its central nervous system penetration. A phase III trial comparing an extended schedule of temozolomide with a standard dose of single-agent DTIC failed, however, to show any statistical differences in terms of response rates, progression-free survival, and overall survival (OS; refs. 3, 4). Temozolomide produces response rates of 4.13% and a median progression-free survival of 1.9 months in patients without brain metastases. More recently, advances in understanding the genetic changes associated with melanoma development identified activating mutations in the serine/threonine kinases BRAF (5), establishing mitogen-activated protein kinase signaling pathways as new drug targets in melanoma. Sorafenib, a multikinase inhibitor of VEGF receptor (VEGFR), KIT, platelet—derived growth factor receptor (PDGFR), and RAF proteins as well as several proangiogenic tyrosine kinases, was tested in phase II trials alone or in combination with carboplatin and paclitaxel and seemed to be promising on response rates and median progression-free survival, but was associated with toxicity (6). Unfortunately, subsequent phase III trials of the combination of sorafenib and paclitaxel/carboplatin only demonstrated benefit in patients with metastatic melanoma in first and second line of therapy (7, 8). Next, even before the era of more specific BRAF inhibitors, Amaravadi and colleagues conducted a phase II trial combining temozolomide with sorafenib in advanced melanoma, showing relative safety and activity in patients without prior history of temozolomide (9).

Authors' Affiliations: [1]Cancer Institute Gustave Roussy; Departments of [2]Epidemiology and Statistics and [3]Dermatology; [4]Stabilité génétique et oncogenèse UMR 8200; [5]Clinical Oncology, Melanoma Branch, Cancer Institute Gustave Roussy; [6]Department of BioPathology, Translational Research Laboratory and Biobank, Institute Gustave Roussy; [7]Institut National de la Santé et de la Recherche Medicale (INSERM), U1015; [8]Center of Clinical Investigations CBT507, Biotherapy, Villejuif; [9]INSERM U1102, Institut de Cancérologie de l'Ouest, Saint Herblain; [10]INSERM, U892, Institut de Recherche Thérapeutique, Nantes; [11]INSERM, U1016, Saint Vincent de Paul Hospital; [12]INSERM U1016, CNRS UMR8104, Cochin Institute; [13]Faculté Paris Sud-Université Paris XI, Paris, France; and [14]IRCCS San Matteo University Hospital Foundation, Pavia, Italy

American Association for *Cancer Research*

In parallel, attempts to harness antitumor immunity have progressively led to therapeutic success in melanoma (10). Anti-CTLA-4 antibodies alone or together with peptide-based vaccination or with DTIC significantly prolonged survival of stage III/IV melanoma in two phase III trials (10, 11). One surmises that in patients responding to immunotherapy, tumor- and/or vaccine-specific T cells reset local tumor microenvironment and convert immune tolerance into immune-related tumor destruction (12).

Because vaccines showed some unexpected efficacy after tumor progression with cytotoxic compounds (13, 14), a new concept emerged whereby the host immune system could contribute to the beneficial effects of cytotoxic compounds (15). Indeed, the outcome of chemotherapy can be influenced by the host immune system at multiple levels. Chemotherapy can kill cancer cells in a way that they elicit an immune response (16) or, alternatively, increase their susceptibility to immune attack (17). In addition, chemotherapy can stimulate anticancer immune effectors either directly (by activating effector or dendritic cells) or indirectly by subverting immunosuppressive mechanisms (18, 19). Hence, a recent report pointed out that patients with metastatic melanoma responding to DTIC exhibit a stromal and immune signature, defined by hallmarks of T-cell infiltration and MHC class II expression (20).

A number of immune effectors, including dendritic cells, T cells, and natural killer (NK) cells, have been involved in natural or therapy-induced tumor immunosurveillance in mice (21, 22). The NK group 2D (NKG2D), a lectin-like activating receptor, markedly influences IFN-γ release and cytotoxic responses upon tumor recognition, exerting selective pressure on transformed cells (23). A large body of preclinical work highlighted the beneficial role of the activating receptor NKG2D in immunosurveillance against cancer (24, 25). In most instances, NKG2D-induced effects are mediated through NK or CD8^{+} effector T cells. Here, we unveil the immunomodulatory role of a multi-tyrosine kinase inhibitor, sorafenib, on a rare subset of circulating (and intratumoral) CD4^{+}CD8^{dim}NKG2D^{+} T cells prone to secrete Th1 cytokines upon cotriggering of CD122 (IL-2/IL-15Rβ chain) and NKG2D receptors. Indeed, sorafenib induced the upregulation of interleukin (IL)-15Rα expression on tumor cells *in vitro* and *in vivo*, and/or on circulating monocytes in metastatic melanoma (cotreated with temozolomide) in a phase I/II prospective trial. In all patients with metastatic melanoma, melanoma expressed high intrinsic levels of MHC class I–related chain A/B (MICA/B) molecules. Patients developing enhanced frequencies of CD4^{+}NKG2D^{+} T cells after two cycles of sorafenib exhibited prolonged survival. Of note, such CD4^{+}NKG2D^{+} T cells failed to dictate the prognosis in another cohort of metastatic melanoma enrolled in a MAGE3 protein (26) underscoring the immunoregulatory role of sorafenib.

Materials and Methods

Patients and treatment plan

SORAFTEM. Sixty-three patients older than 18 years of age, with histologically confirmed metastatic or unresectable melanoma, measurable disease, an Eastern Cooperative Oncology Group performance status less than 2, with adequate hematologic, renal, hepatic, and coagulopathic functions, were included in a phase I/II investigator-sponsored study SORAF-TEM (European Union Drug Regulating Authorities clinical trial EudraCT 2007-000527-18). The number of prior therapies is summarized in Table 1. Patients had discontinued their earlier systemic therapy at least 4 weeks before entering the trial. Previous brain radiotherapy was allowed, provided patients were not clinically symptomatic. The study protocol

Table 1. Characteristics of patients ($n = 63$)

Gender (male/female)	35/28
Age (mean $\pm$ SD) [range]	48.5 $\pm$ 13.8 [22–75]
Type	
SSM	20
Nodular	12
Lentigo maligna	1
Acral lentiginous	2
Mucosal	7
Ocular	4
Other	17
Metastasis (56 patients have metastases)	
Number of metastasis lesions per patient (mean $\pm$ SD)	5.1 $\pm$ 2.0 [1–10]
Metastatic sites	
Nodes	40
Liver	11
Lung	22
Peritoneum	8
Skin	19
Bone	7
Muscle	4
LDH level U/L (mean $\pm$ SD) [range]	341 $\pm$ 478 [90–3,500]
LDH $\leq$ 250 U/L	34
LDH > 250 U/L	23
ND	6
Treatment schedule	
sorafenib 400 mg/d, temozolomide 100 mg/m^2	3
sorafenib 400 mg/d, temozolomide 150 mg/m^2	6
sorafenib 800 mg/d, temozolomide 150 mg/m^2	54
Previous chemotherapy	
No	9
One line	22
Two lines	19
Three lines	10
Four lines	3
3-month evaluation	
Responders	26
Nonresponders	37

Abbreviations: SSM, spreading superficial melanoma; ND, not determined.

was approved by the Institutional Review Boards at the University of Kremlin Bicêtre (Paris, France) and Institut Gustave Roussy (Villejuif, France). All patients provided informed consent before enrollment. The treatment plan is outlined in Supplementary Fig. S1. Stage III and IV melanoma-bearing patients were enrolled from 2006 to 2009 in a dose-escalating phase I followed by a phase II extension cohort at the maximum-tolerated dose trial testing the efficacy of the combinatorial regimen of temozolomide (Schering Plough; 100–150 mg/m^2 daily for 7 days every 2 weeks) and sorafenib (Bayer; 400–800 mg twice daily without interruption). Therapy was continued until disease progression or intolerable toxicity. Response assessments consisted of physical examination every 4 weeks together with computed tomography scans of the chest, abdomen, and pelvis every 8 weeks. Patients were assessed by an investigator using the Response Evaluation Criteria in Solid Tumors (RECIST) guidelines 1.1. Responses were confirmed by follow-up radiographic evaluation 4 weeks after the initial response criteria were met. BRAF mutations were determined according to technical methods previously described (9). The primary endpoint of the trial was the efficacy of the treatment at 3 months. Patients were classified as objective response or stabilization (called "responders" henceforth) versus progressive disease or death (PD; called "nonresponders" henceforth).

MAGE3 protein–based vaccines. The details about patient characteristics, protocol description, and survival have been previously reported by Kruit and colleagues (26). CD4$^+$ NKG2D$^+$ T cells were analyzed at in the beginning before vaccine inoculation (1 month after relapse with conventional therapies) and correlated with OS.

NY-ESO-1 vaccine trial. Prevaccine peripheral blood samples were collected from patients with malignant melanoma, sarcoma, breast, and ovarian cancer enrolled in a clinical trial of vaccination with recombinant NY-ESO-1, Montanide ISA 51, and CpG 7909 (27) upon informed consent and approval by the Institutional Review Board of Columbia University Medical Center (New York, NY).

Immunohistochemistry studies

Paraffin-embedded tumor tissues were first rehydrated and then treated with hydrogen peroxide (H$_2$O$_2$; DAKO) for neutralizing endogenous peroxidase and Serum Free Protein Block (DAKO) to prevent nonspecific binding. After blocking, primary antibody, anti-MICA/B (SR99; a kind gift from Sophie Caillat-Zucman, INSERM, U1016, Saint Vincent de Paul Hospital, Paris, France) was applied. Binding specificity was controlled by immunoglobulin G (IgG)1-isotype controls (RnD). For visualization, EnVision anti-mouse (DAKO) horseradish peroxidase–conjugated streptavidin was applied, followed by the chromogen 3,3′-diaminobenzidine/H$_2$O$_2$ (DAB; DAKO). Immunostained sections were counterstained very briefly with Mayer's Hemalaun, dehydrated, and cleared with xylene, before covered with mounting medium (toluene-based) and coverslips (DAKO). For staining of anti-CD3 (polyclonal rabbit, 1:150; DAKO), anti-CD4 (1:20; Novocastra), and anti-CD8 (1:25; Novocastra), the Benchmark system was used. For detection of IL-15Rα, primary antibody (AF247; R&D Systems) was applied at

10 µg/mL after blocking, and anti-goat IgG Alexa Fluor 568 was used at 5 µg/mL as secondary antibody. Isotype-matched antibody was used as negative controls. Samples were mounted in ProLong Gold antifade with 4′,6-diamidino-2-phenylindole (DAPI) reagent (Molecular Probes). Fluorescent images were analyzed with an epifluorescent microscope (Zeiss Apotome Microscope).

PBMC preparations

Blood samples were drawn from 63 patients before and after each treatment cycle and from 12 healthy volunteers. Peripheral blood mononuclear cells (PBMC) were resuspended in culture medium, i.e., RPMI-1640 (GIBCO Invitrogen), 10% human AB$^+$ serum (Jacques Boy), 1% penicillin/streptavidin (PEST; GIBCO Invitrogen), and 1% 2 mmol/L glutamine (GIBCO Invitrogen). Some cells were then stained for flow-cytometric analyses and the rest were resuspended in CryoMaxx medium (PAA Laboratories) for storage in liquid nitrogen.

Tumor-infiltrating lymphocytes preparations

Resected lymph node specimens and/or metastatic tissue from 16 patients with metastatic melanoma were analyzed for infiltrating lymphocytes. Tissue samples were placed in dissociation medium, i.e., RPMI-1640, 1% PEST, collagenase IV (8,000 UI/mL), hyaluronidase (112,000 IU/mL), and DNAse (12,700 IU/mL), and run on a gentleMACS dissociator (Miltenyi Biotec). The cell samples were then diluted in RPMI-1640 + 10% human AB$^+$ serum, passed through a cell strainer, and centrifuged for 10 minutes at 300 $\times$ g. Next, the cells were resuspended in PBS and stained for flow-cytometric analyses. Tumor-coupled specimens of noninvaded lymph node or blood samples were obtained from 10 patients and were analyzed as above.

Flow cytometry

Cells were stained with fluorochrome-coupled monoclonal antibodies (mAb), incubated for 20 minutes at 4°C, and washed. Adherent cells were treated with trypsine (Gibco) before the staining step. Cell samples were analyzed using a CyAn ADP 9-Color flow cytometer (Beckman Coulter) or an LSRII flow cytometer (BD Biosciences). For proper compensation, single-stained antibody-capturing beads were used (CompBeads; BD Biosciences). Data were analyzed using FlowJo (TreeStar, Inc.) or FACSDiva (BD Biosciences). For accurate determination of nondiscrete populations, fluorescence-minus-one (FMO) controls were used. For dead-cell discrimination, DAPI (Invitrogen) or the fixable amine-reactive LIVE/DEAD Cell-Stain Kit (Invitrogen) was used. For phenotypic analysis of CD4$^+$NKG2D$^+$ T cells, PBMC samples from 11 patients were thawed and resuspended in PBS for 9-color flow-cytometry staining. T cells of interest were identified by CD3, CD4, CD56, CD8, CD14, and NKG2D mAbs and costained with CD28 and CD45RA, or 2B4 and CD161, or IL-15Rα and CX3CR1, or CD25 and CD158 antibodies. The following fluorochrome-coupled anti-human mAbs were used: anti-CD3 (Miltenyi Biotec, BD, Beckman Coulter), anti-CD4 (BD), anti-CD8 (BD, eBioscience), anti-CD14 (BD, eBioscience), anti-CD56 (Beckman Coulter), anti-NKG2D (Miltenyi Biotec), anti-Foxp3

(eBioscience), anti-CD25 (BD), anti-CD28 (BD), anti-CD45RA (BD, eBioscience), anti-2B4 (BD), anti-CD161 (Beckman Coulter), CD158a (BD), anti-CX3CR1 (MBL), and anti-Ki67 (BD). Rabbit polyclonal anti-IL-15Rα IgG antibody was purchased from Santa Cruz Biotechnology. Purified anti-CD3 (OKT3), anti-NKG2D (AF750), and goat anti-rabbit IgG-allophycocyanin (APC) were purchased from BioLegend.

T-cell purification and functional assays

Frozen PBMC samples were quickly thawed, washed, and resuspended in recommended medium (RoboSep Buffer; STEMCELL Technologies) for magnetic bead separation with the EasySep Human CD4-Positive Selection kit (STEMCELL Technologies). Positive-selection kit was chosen to avoid depleting $CD8^+$ $CD4^+NKG2D^+$ T cells. For isolation of $CD4^+NKG2D^+$ T cells and $NKG2D^+$ NK cells, previously frozen PBMCs were stained with mAbs to CD3, CD4, CD56, CD14, and NKG2D and sorted by flow cytometry on a three-laser MoFlo XDP cell sorter (Beckman Coulter), or a three-laser ARIA III cell sorter (BD). More than 98% pure populations of $CD3^+/CD4^+/NKG2D^+/CD56^-/CD14^-$ and $CD56^+/NKG2D^+/CD3^-/CD4^-/CD14^-$ cells were obtained.

Cytokine production. PBMCs from patients with metastatic melanoma were thawed and resuspended in culture medium, and kept at 37°C, overnight. The next day, cells were enriched for $CD4^+$ T cells and seeded at 10^6 cells/mL on a flat-bottomed Nunc MaxiSorp 96-well plate, precoated with or without anti-CD3 antibody (0.5 μg/mL), anti-CD122 antibody (1, 10 μg/mL), and anti-NKG2D antibody (4 μg/mL) alone or in combination. After 20 hours of cell culture, the supernatant was collected, cleared by centrifugation, and analyzed by ELISA for quantification of IFN-γ (BD), IL-2 (BD), TNF-α (BD), IL-17 (R&D Systems), and IL-10 (BD) according to the instruction manuals. For cytokine-release from purified cells, fluorescence-activated cell sorting (FACS)-sorted $CD4^+NKG2D^+$ T cells and NK cells were cultured overnight in the presence or absence of soluble MIC (sMICA; 5 ng/mL; a kind gift from Sophie Caillat-Zucman) and recombinant IL-15 (rhIL-15; 5 ng/mL; R&D Systems) alone or in combination. Release of IFN-γ into the supernatant was then measured by ELISA according to the manufacturer's instructions.

Proliferation. After precoating UV-sterilized MaxiSorp Nunc plates with or without anti-CD3 antibody (1 μg/mL), we plated $CD4^+$ T cells in the presence or absence of sMICA (5 ng/mL) and IL-15 (5 ng/mL) alone or in combination. Cells were then cultured for 5 days, and then harvested for staining with the phycoerythrin (PE)-coupled Ki67, as well as other surface mAbs.

Cytotoxicity. PBMCs were cultured in RPMI/10%SAB with or without 20 ng/mL IL-15 for 4 days. One day before coculture, MEL10 target cells were stained with CMTMR (Invitrogen), seeded on a round-bottomed plate (10,000 cells/well), and treated with or without sorafenib (10 μmol/L). The next day, PBMCs were collected and enriched for CD4 cells before FACSAria III-sorting of NKG2D-positive/negative cells. Target cells were washed with PBS before adding 40,000 sorted T cells to each well and cultured for 20 hours. Floating cells were then transferred to FACS tubes and adherent cells were trypsinized

and collected into the same tubes. After centrifugation, the cells were resuspended in PBS and analyzed on a FACSCanto II (BD). For cell death determination, To-Pro-3 (Invitrogen) was added to the tube just before running.

Exposure of melanoma cells to cytotoxic compounds

Eight human melanoma cell lines, M14, M96, MELP, MEL8, MEL397, MEL888, MT10, and MZ2 were plated and grown confluent in Dulbecco's Modified Eagle Medium (DMEM) medium (GIBCO Invitrogen) supplemented with 10% FBS (PAA Laboratories), and 1% PEST. Cells were then cultured in the presence or absence of sorafenib (5 μmol/L, Nexavar; Bayer) and temozolomide (50 μmol/L, Temodal; Schering Plough) alone or in combination (protocol without cell death, not shown). The next day, cells were collected and labeled with IL-15Rα polyclonal antibody (H107) followed by an APC-coupled secondary antibody and then stained with DAPI for dead-cell exclusion for flow cytometry analysis. FMO tube was added as negative control, and background staining was excluded with a goat anti-rabbit IgG-APC.

Quantitative reverse transcription PCR for IL-15Rα isoforms

Total cellular RNA was isolated from melanoma cells with the RNeasy Kit (Qiagen). First-strand cDNA was synthesized from 1 μg of total RNA using SuperScript III Reverse Transcriptase (Life Technologies) and random primers according to the manufacturer's instructions. The quantitative reverse transcription PCR (qRT-PCR) for IL-15Rα (Hs00542604_m1, Hs01986843_m1, and Hs00233692_m1) isoforms and for β2-microglobulin was performed by real-time fluorescence measurement using StepOnePlus System (Life Technologies). The qRT-PCR data were adjusted to β2-microglobulin measurements using the $2^{-\Delta C_T}$ method (28).

Microarray

Global gene expression analysis was performed on 20 cDNA samples from biopsies of patients with melanoma prior and post two cycles of sorafenib/temozolomide, using the Human Gene Expression 8 × 60 K Agilent Human Microarray Kit. Functional analysis was carried out through the Ingenuity Pathway Analysis (Ingenuity System).

Statistical analyses

Differences between groups of quantitative data were assessed by Mann–Whitney U test or Wilcoxon signed-rank test for all distributions, or Student paired or unpaired t test if the criteria for Gaussian distribution was met. All reported P values were two-sided, and a P value of less than 0.05 was considered statistically significant.

Results

Effector memory $CD4^+NKG2D^+$ T cells in metastatic melanoma patients

In accordance with a previous report (9), the sorafenib and temozolomide combination therapy (schedule summarized in Supplementary Fig. S1) induced one complete response (CR), four partial responses (PR), and 21 disease stabilizations (SD)
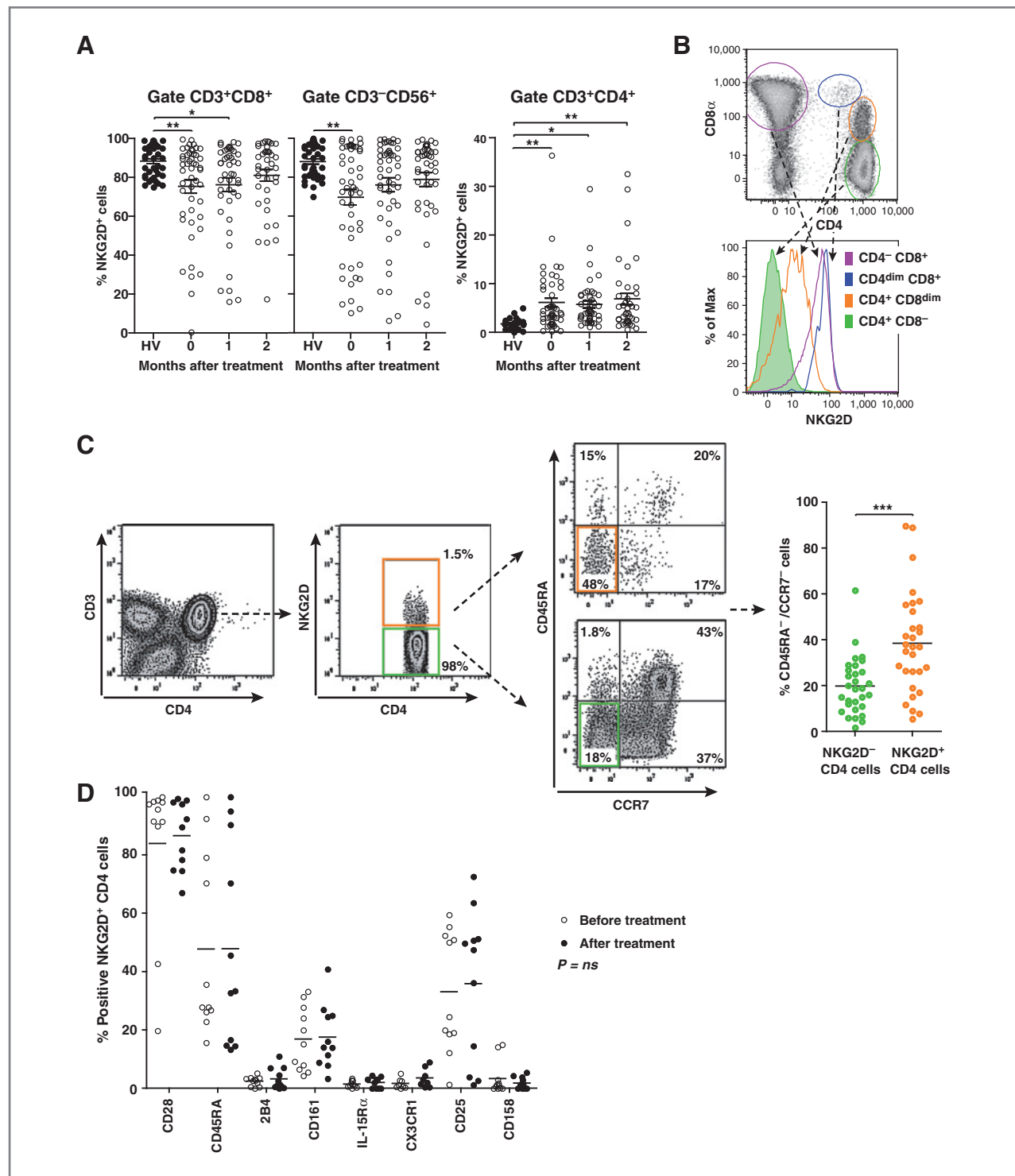
Figure 1. Increase of CD4$^+$NKG2D$^+$ T cells exhibiting an T$_{EM}$ phenotype. A, flow cytometry analyses of NKG2D expression on freshly isolated subsets of circulating lymphocytes [CD3$^+$CD8$^+$ (left), CD3$^-$CD56$^+$ (middle), and CD3$^+$CD4$^+$ (right)] in metastatic melanoma before (0) and after one to two cycles (1, 2) of therapy as well as in sex- and age-matched healthy volunteers (HV). Each dot represents 1 patient or healthy volunteer. Intraindividual variations between pre- and posttherapy are analyzed by paired Student t test (*, $P < 0.05$; **, $P < 0.01$). B, flow cytometry analyses of NKG2D expression according to CD4 and CD8 expression. NKG2D expression on CD4$^+$ T cells proportional to the staining with anti-CD8 mAb shown in a representative histogram (right). C and D, phenotyping of CD4$^+$NKG2D$^+$ T cells recovered from metastatic melanoma at diagnosis according to CD45RA and CCR7 expression (C) or from 11 patients with metastatic melanoma in a kinetic study according to various NK cell receptors (D). Student t test to compare CD4$^+$NKG2D$^+$ or NKG2D$^-$ T cells; ***, $P < 0.001$. Intraindividual variations between pre- and posttherapy are analyzed by Wilcoxon signed-rank test (ns, not significant).
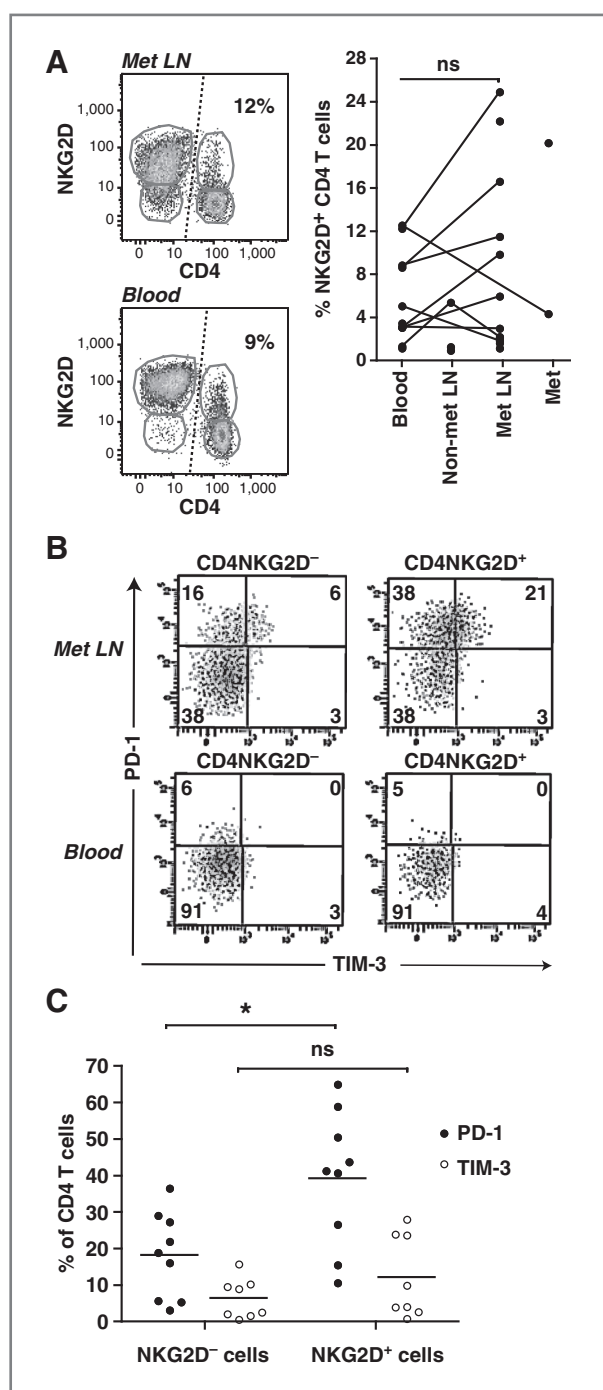
Figure 2. Phenotype of CD4$^+$NKG2D$^+$ tumor-infiltrating lymphocytes in metastatic melanoma. A, flow cytometry analyses of CD45$^+$CD3$^+$CD4$^+$ infiltrating lymphocytes in blood, noninvaded lymph node (Non-met LN), lymph node metastasis (Met LN), or other metastatic tissue (Met). A representative dot plot is shown with the percentages of NKG2D$^+$ cells among the CD4$^+$ T-cell population (left two). In 9 cases, paired specimen [coupling blood or noninvaded lymph node to tumor beds (Met lymph node or Met)] were examined (connected lines, right). Wilcoxon signed-rank test showed no statistical significance (ns). B and C, expression of PD-1 and Tim-3 on CD45$^+$CD3$^+$CD4$^+$ tumor-infiltrating lymphocytes (Met LN) versus PBMCs (Blood) based on NKG2D expression. A representative dot plot (B) is shown and the results from 9 Met lymph nodes are depicted in the graph (C). Student t test was used to compare CD4$^+$NKG2D$^+$ and NKG2D$^-$ T cells; *, $P < 0.05$; ns, not significant.
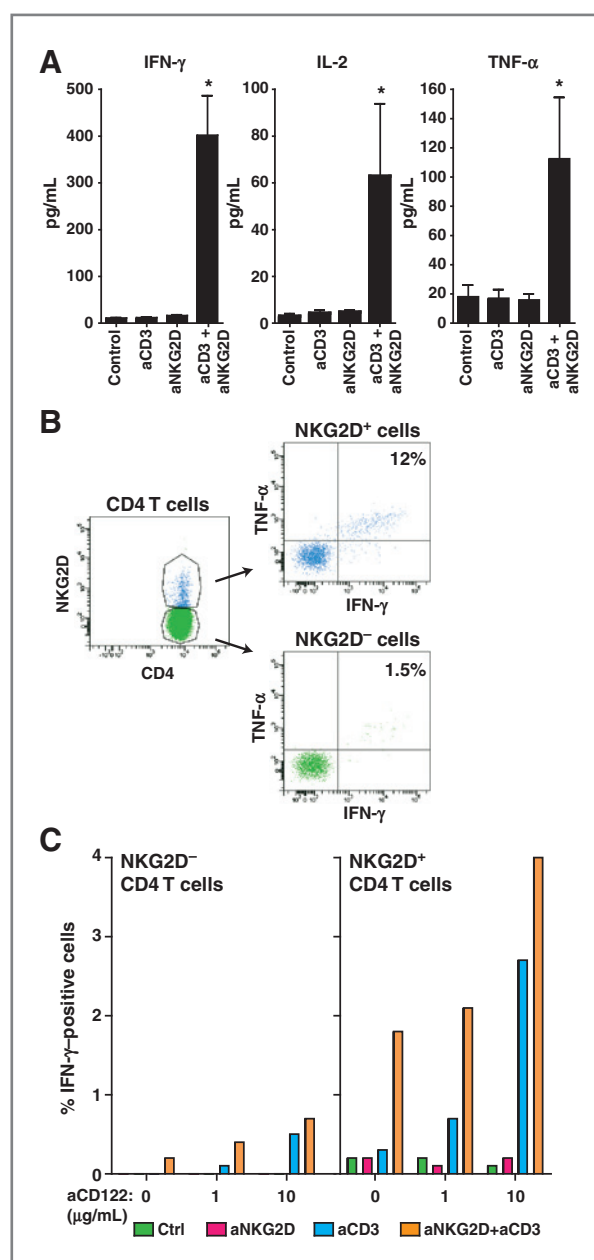

Figure 3. Synergistic effects of TCR, CD122, and NKG2D engagement for Th1 polarization in CD4$^+$NKG2D$^+$ T cells. A, TCR and NKG2D-dependent Th1 cytokine release by CD4$^+$NKG2D$^+$ T cells. Cytokine release was measured using ELISA for human IFN-γ, IL-2, and TNF-α in the supernatants of circulating CD4$^+$ T cells recovered before therapy in 4 patients with metastatic melanoma. Cells were stimulated overnight with a combination of suboptimal amounts of anti-CD3 (aCD3; 0.5 µg/mL) and anti-NKG2D (aNKG2D; 4 µg/mL) antibodies. IL-17 and IL-10 were not detectable in these conditions (not shown). The graph depicts the means + SEM of cytokine release from four metastatic melanoma (each one being tested in triplicate wells). The synergistic effect of aCD3 + aNKG2D was tested by Student t test (*, $P < 0.05$). B, cytokine production, gating on CD4$^+$NKG2D$^+$ (top) and CD4$^+$NKG2D$^-$ (bottom) at 48 hours of stimulation using flow cytometry and intracellular stainings. A representative dot plot is depicted. C, the synergistic effect of CD122 triggering (dose response of cross-linked anti-CD122 agonistic antibody) together with TCR/NKG2D engagement on cell-sorted CD4$^+$NKG2D$^+$ or NKG2D$^-$ T cells from 3 patients with metastatic melanoma. Data from one representative patient show the percentage of IFN-γ^+ cells assessed by flow cytometry and intracellular staining.

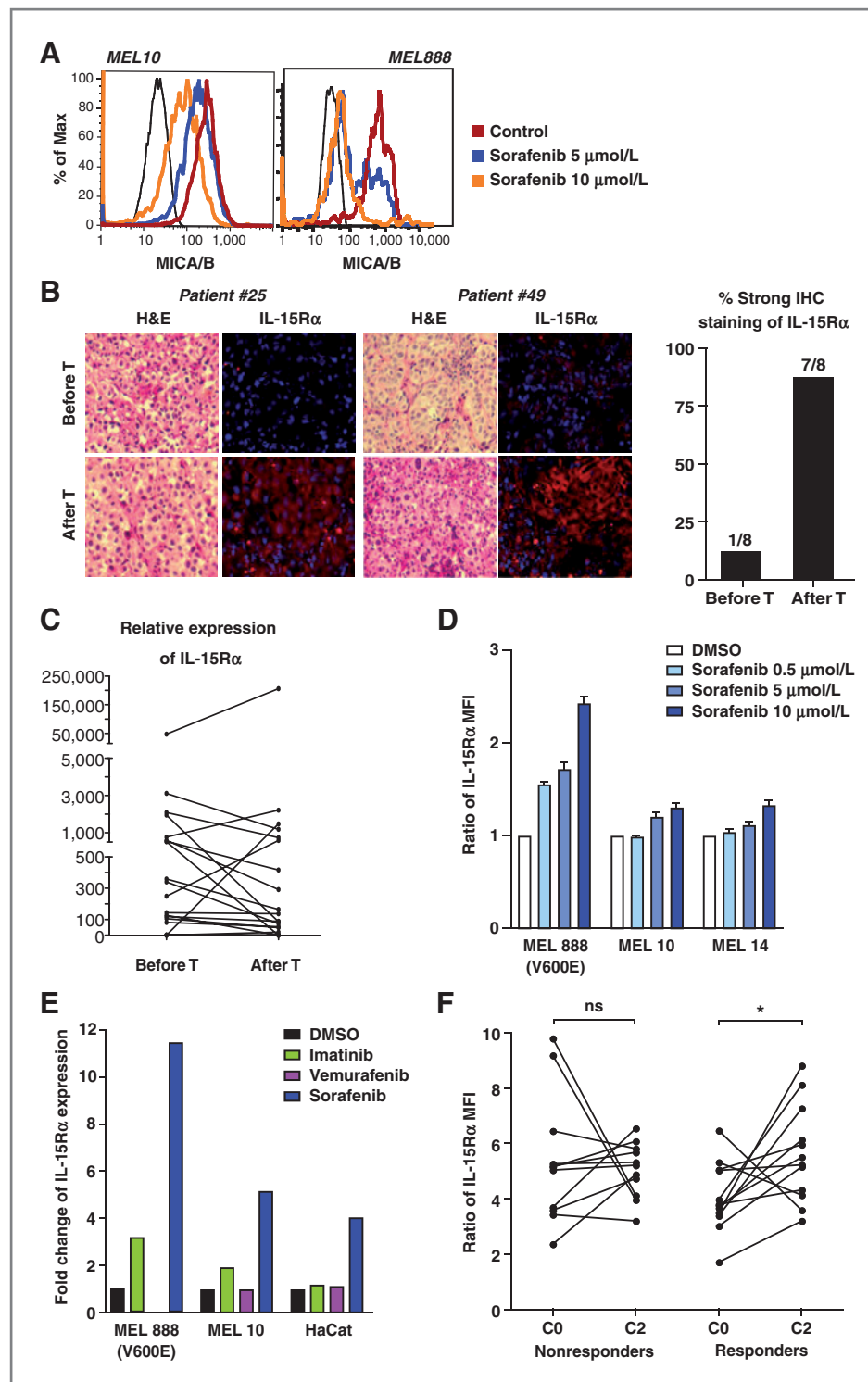**Figure 4.** Sorafenib-induced cell surface expression of IL-15Rα and downregulation of MICA/B. A, downregulation of MICA/B expression on melanoma cell lines *in vitro*. Flow cytometry analysis of MICA/B expression at 48 hours after exposure to sorafenib at increasing concentrations gating on live MEL10 and MEL888 cells. FMO-control is indicated in thin black line. Representative overlays are shown. B, hematoxylin and eosin (H&E) staining of metastatic melanoma lesions and immunofluorescence using anti-IL-15Rα antibodies. Nuclei are visualized with a DAPI (blue) staining, whereas melanoma plasma membrane appears in red (staining with secondary anti-goat IgG Alexa Fluor 568 recognizing the anti-IL-15Rα antibody). Two representative patients' paired lesions (pre- and posttherapy) are shown. Right, graph representative of 8 independent tumor lesions examined before and after therapy, showing the percentage of positivity. C, RT-PCR determinations of the relative expression of the IL-15Rα gene in 20 paired metastatic melanoma lesions before and after three cycles of therapy. (*Continued on the following page.*)

at 3 months (CR+PR+SD called hereafter "responders") and 37 progressive disease being referred to as "nonresponders" according to the RECIST criteria (Table 1). Severe lymphopenia was observed in both responders and nonresponders (Supplementary Fig. S2A and S2B).

We phenotyped circulating lymphocytes in a longitudinal study over 2 months in 63 patients included in this phase I/II trial. All patients with metastatic melanoma showed a significant reduction of NKG2D expression in both CD8^{+} T and NK cells at diagnosis compared with healthy volunteers (Fig. 1A). Conversely, there was a higher proportion of CD4^{+} T cells expressing NKG2D in all patients with metastatic melanoma compared with healthy volunteers (Fig. 1A, right). These CD4^{+}NKG2D^{+} T cells differed from the CD4^{+}NKG2D T-cell subset in that they coexpressed low levels of CD8αβ (Fig. 1B) and exhibited an effector memory (T_{EM}; CD45RA^{−}CCR7^{−}) phenotype (Fig. 1C). Extensive phenotyping showed that about 20% of CD4^{+}NKG2D^{+} T cells expressed the C-type lectin receptor NKR-P1A (CD161) as described by others (29), but failed to express other NK receptors (such as 2B4, KIR, NCR, and CD94/NKG2A) in contrast to previously described CD4^{+}NKG2D^{+} T cells (Fig. 1D; ref. 30). Finally, CD4^{+}NKG2D^{+} T cells did not express the fractalkine receptor CX3CR1 associated with T-cell trafficking into tumor beds (Fig. 1D).

Lymph node resection in high-grade melanoma allowed us to examine the capacity of CD4^{+}NKG2D^{+} T cells to traffic to tumor beds. Indeed, this subset represented up to 2% to 25% of the CD4^{+} tumor-infiltrating lymph node T cells (Met lymph node), generally not enriched compared with blood or nonmetastatic lymph node (non-Met lymph node; when paired specimen were available; Fig. 2A), and expressed higher levels of PD-1 (but similar levels of TIM-3) molecules compared with NKG2D^{−} CD4^{+} T cells (Fig. 2B and C). Of note, these Met lymph node contained about 73% ± 20% of CD45^{−} cells.

Altogether, the regulation of NKG2D expression in CD4^{+} versus CD8^{+} or NK cells is uncoupled in patients with metastatic melanoma. The accumulation of CD4^{+}CD8^{dim} or CD4^{+}NKG2D^{+} T-cell subset in blood (and tumors) is frequently observed in melanoma but can also be found in other malignancies (Supplementary Fig. S3).

Th1 polarization of CD4^{+}NKG2D^{+} T cells upon engagement of NKG2D and CD122

First, we analyzed the capacity of CD4^{+} T cells to secrete cytokines after engagement of the T-cell receptor (TCR) and/or NKG2D before therapy. A strong synergistic effect on the production of IFN-γ, IL-2, and TNF-α was observed when both receptors were triggered (Fig. 3A) in responders as well as in nonresponders (not shown). Importantly, upon TCR and NKG2D triggering, this subset failed to produce IL-17 or IL-10 (not shown). Intracellular staining revealed that most CD4^{+} NKG2D^{+} T cells produce both IFN-γ and TNF-α (Fig. 3B). Because IL-15 has been shown to be a key factor in arming an NKG2D-dependent activation of TCRαβ CTLs in celiac disease (31), we addressed whether purified CD4^{+}NKG2D^{+} T cells could be activated by coengagement of NKG2D and/or CD122 (IL-2Rβ common to both IL-2/IL-15 signaling) with a suboptimal cross-linking of CD3 molecules. Although CD4^{+}NKG2D^{−} T cells failed to release IFN-γ upon receptor engagement, cell-sorted CD4^{+}NKG2D^{+} T cells produced high levels of Th1 cytokines after a combined stimulation through TCR, CD122, and NKG2D (Fig. 3C). To further characterize the functions of these cells, we performed three additional assays (Supplementary Fig. S4). First, we incubated the NKG2D^{+} or NKG2D^{−} cell subset with soluble MICA (sMICA; expected to trigger NKG2D) and rhIL-15 (expected to stimulate IL-2Rβγ) in vitro in the presence or absence of a TCR engagement. Interestingly, sMICA+IL-15 could independently of TCR engagement synergistically induce IFN-γ secretion in the CD4^{+}NKG2D^{+} T-cell subset (as in NK cells) but not in CD4^{+}NKG2D^{−} T cells (Supplementary Fig. S4A). However, proliferation of either NKG2D^{+} or NKG2D^{−} CD4^{+} T cells could only be induced after CD3 cross-linking (Supplementary Fig. S4B). In contrast to their NKG2D^{−} counterparts, the CD4^{+}NKG2D^{+} effectors were also able to recognize and kill melanoma cells (MEL10 cell line) after IL-15 priming (Supplementary Fig. S4C). Sorafenib exposure did not enhance their cytotoxicity, which might be explained by the reported direct inhibitory activity of sorafenib on T-cell functions (32). Moreover, as shown in Fig. 4, IL-15Rα expression was only weakly increased (Fig. 4D) on the cell surface of MEL10 cells by sorafenib treatment (Fig. 4E), which could explain why the addition of IL-15 to engage CD122 was mandatory for the MEL10 cell line. To follow up on this, we then switched to the melanoma cell line MEL888, of which sorafenib had shown greater impact on the expression of IL-15Rα both on mRNA levels and cell surface (Fig. 4E and D), and tested the activation of CD4^{+}NKG2D^{+} T cells without the addition of exogenous rhIL-15 in the presence of sorafenib-treated or -untreated MEL888 cells. The result showed that CD4^{+}NKG2D^{+} T cells could only secrete IFN-γ in the presence of sorafenib-treated MEL888 cells (Supplementary Fig. S4D).

Thus, CD4^{+}NKG2D^{+} T lymphocytes constituted an T_{EM} Th1-polarized T-cell subset capable of releasing cytokines upon TCR engagement with a strong costimulatory activity of the NKG2D receptor or upon coengagement of CD122 and NKG2D receptors.

(Continued.) D, flow cytometry analyses of IL-15Rα expression on three melanoma cell lines after in vitro exposure to increasing dosing of sorafenib. Ratio of mean fluorescence intensity (MFI) between FMO-control and specific stainings is shown after an overnight culture in control medium with DMSO, sorafenib (with a dose response), and/or temozolomide (at 50 μmol/L, not shown, but no upregulation). Each determination was performed twice with similar results. E, fold change RT-PCR of IL-15Rα gene expression after an 18-hour incubation of three cell lines with imatinib (1 μmol/L), vemurafenib (10 μmol/L), or sorafenib (10 μmol/L) at doses triggering significant cell death or proliferation arrest. DMSO was used as control. F, IL-15Rα protein expression, monitored on CD14^{+} PBMCs, in nonresponding (NR; $n = 11$; left) and responding (R; $n = 12$; right) patients. For each patient, specific IL-15Rα staining and FMO control were performed at baseline (C0) and after two cycles (C2) of sorafenib/temozolomide. The dots represent the ratio of the MFI of the specific IL-15Rα signal to the MFI of the FMO control for each patient at C0 and C2. *, $P < 0.05$; ns, not significant using Wilcoxon signed-rank test.

Table 2. Semiquantitative assessment of CD3, CD4, CD8, and MICA infiltrates by IHC

Patients[a]	Clinical response	Before therapy[b]				After therapy[b]			
		CD3	CD4	CD8	MICA/B	CD3	CD4	CD8	MICA/B
13	R	++	+/−	++	++	++	+	++	+
26	R	−	−	−	++	+	−	−	+
34	NR	+	−	−	+	+	−	−	+
38	NR	+	−	−	++	+	−	−	++
40	R	+	+	+	+	+	+	+	+
41	R	++	+	+	+	++	+	+	+
47	NR	+	−	−	+	+	−	−	+
48	NR	+	−	++	++	+	−	+	++
49	NR	+	−	++	+	++	−	++	+

Abbreviations: R, responder; NR, nonresponder.
[a]Inclusion number.
[b]Staining estimations assessed by two independent pathologists: −, no staining; +/−, weak; +, intermediate; ++, strong.

Regulation of IL-15Rα expression by sorafenib in tumor beds

We analyzed how sorafenib or temozolomide could modulate the expression of the ligands for these receptors *in vitro* and *in vivo*. Lymph node–residing melanoma was reported to express low levels of NKGD ligands (33). We analyzed sixteen "paired" but independent tumors (mostly from subcutaneous lesions), before and after three cycles of therapy by immunohistochemistry of paraffin-embedded melanoma. First, anti-CD3, -CD4, and -CD8 antibody stainings revealed abundant infiltrates that were not significantly altered by therapy (Table 2 and Supplementary Fig. S5). The SR99 antibody recognizing MICA/B revealed that the intensity of the staining seemed moderate to strong on plasma membrane and in the cytosol in all specimens regardless of the location (Supplementary Fig. S5 and Table 2). Of note, no staining was observed in the epidermal or mesenchymal cells of normal skin adjacent to the melanoma (not shown). The expression of MICA/B proteins was maintained by the therapy in tissue sections (Table 2) although sorafenib could, with increasing concentrations, downregulate MICA expression on melanoma cell lines *in vitro*, especially on MEL888 cells (Fig. 4A). Note that treating the MEL888 cells with 10 μmol/L sorafenib for 24 hours led to the release of sMICA/B in the supernatant (not shown).

We also monitored the IL-15Rα expression on tumor cells. Immunofluorescence analyses of paired melanoma pre- and posttherapy using anti-IL-15Rα–specific antibodies revealed that in most cases (7 of 8 patients), therapy increased cell-surface expression of IL-15Rα on tumor cells (Fig. 4B). RT-PCR analyses of 20 tumor biopsies compared the relative expression of the IL-15Rα gene pre- versus posttherapy and confirmed, in 4 cases, the upregulation of transcription or a strong and stable basal expression in 2 cases (Fig. 4C). Corroborating these data, sorafenib induced cell-surface expression of IL-15Rα and enhanced transcription of IL-15Rα in melanoma lines *in vitro* (Fig. 4D). Note

that temozolomide was not able to induce IL-15Rα expression *in vitro* and did not inhibit IL-15Rα expression induced by sorafenib (not shown). Interestingly, B-RAF or c-KIT inhibitors (vemurafenib or imatinib) failed to modulate IL-15Rα in melanoma cell lines *in vitro* (Fig. 4E). Monitoring of IL-15Rα on peripheral blood CD14^{+} cells at baseline and after two cycles of treatment revealed an upregulation preferentially in responding patients (Fig. 4F), and in patients with longer OS (over the median time of survival, 224 days; $P = 0.03$ with Wilcoxon signed-rank test; data not shown).

Microarray analysis was performed on 20 paired biopsies before (day 0) and after treatment (day 21) from 20 patients by establishing the log ratio (day 21/day 0) to identify genes that could be modified by the treatment regardless of the clinical response. This analysis revealed a cluster of genes among which IL-15, STAT5, and STAT1 appeared first as upregulated after treatment (Supplementary Fig. S6). Because of the limited number of samples and the absence of a validation set, it was impossible to perform relevant analysis to distinguish responders from nonresponding patients.

To conclude, sorafenib alone or combined with temozolomide may induce membrane expression of IL-15Rα *in vitro* and *in vivo* in patients with melanoma.

Increase of CD4^{+}NKG2D^{+} T cells associated with OS

Given the sorafenib-induced accumulation of CD4^{+} NKG2D^{+} Th1 cells and IL-15Rα expression in melanoma lesions, we hypothesized that this subset could influence therapeutic outcome. We analyzed potential correlations between the frequencies of CD4^{+}NKG2D^{+} T, CD8^{+}NKG2D^{+} T cells, and CD56^{+}NKG2D^{+} NK cells at various time points with the clinical response evaluated at 2 months and OS. None of these parameters was associated with clinical response at any time points (Supplementary Fig. S2C and data not shown). However, lymphopenia at baseline influenced OS. Considering that median survival of the whole cohort is 227 days, patients

with prolonged survival (>227 days) exhibited higher lymphocyte counts at baseline compared with rapidly progressive patients (Fig. 5A). Importantly, the increase of circulating $CD4^+NKG2D^+$ T cells at two cycles of therapy was associated with prolonged survival, whereas the parallel decrease of $CD8^+$ $NKG2D^+$ or $CD56^+NKG2D^+$ NK cells was not (Fig. 5B and C and Supplementary Fig. S2D). The elevation of $CD4^+NKG2D^+$ T-cell subset observed post-sorafenib (combined with temozolomide) was not apparent after miscellaneous lines of conventional therapies (including DTIC, fotemustine, isolated limb perfusion, vaccines) where long-term or short-term survivors had no more than 2.5% to 3% of $CD4^+NKG2D^+$ T cells (Fig. 5D). Altogether, it is tempting to speculate that the accumulation of $CD4^+NKG2D^+$ Th1 cells may be regulated by a therapy facilitating the exposure of IL-15Rα on tumor cells and/or circulating monocytes.

Discussion

Here, we report the first demonstration that sorafenib (combined with temozolomide) could (i) increase the proportion of a rare subset of T_{EM} $CD4^+NKG2D^+$ Th1 cells, and (ii) induce the upregulation of IL-15Rα on monocytes and/or in tumor sections. NKG2D ligands along with the therapeutic induction of IL-15Rα expression on the plasma membrane of tumor cells (and/or monocytes) could restore/favor the activation of tumor-infiltrating effector lymphocytes. We show that these molecules are either detectable at baseline (MICA expression) or induced by sorafenib (IL-15Rα) in

metastatic melanoma where a subpopulation of rare $CD4^+$ T cells expressing NKG2D is abnormally represented (compared with healthy volunteers). This subset can be induced to proliferate after engaging TCR and NKG2D receptors and to release Th1 cytokines after engaging CD122 and NKG2D receptors.

Several subsets of $CD4^+NKG2D^+$ T cells have been described. First, in patients with cancer, tumor expression and shedding of sMICA/B ligand of NKG2D drove the proliferation of a $CD4^+NKG2D^+$ T cell population that produced IL-10, TGF-β, and FasL (34, 35). The expansion of these cells inhibited bystander $CD8^+$ and $CD4^+$ T-cell proliferation ex vivo. The same autoreactive T-cell subset was inversely correlated with disease activity in autoimmune diseases (such as juvenile-onset systemic lupus erythematosus). In this report, sMIC serum levels were also inversely correlated with disease activity (36). Second, in contrast to this "regulatory" phenotype, a "proinflammatory" and cytolytic $CD4^+NKG2D^+$ T-cell subtype has been described in autoinflammatory diseases such as Wegener's granulomatosis (37, 38), rheumatoid arthritis (39), and Crohn's disease (40). In most of these reports, $CD4^+$ $NKG2D^+$ T cells harbor an effector-memory phenotype and express many other NK-cell activating receptors (such as 2B4, DNAM-1, and CRACC) likely contributing to pathogenesis. Indeed, coligation of 2B4 in combination with DNAM-1 or NKG2D enhanced $CD4^+CD28^-$ T-cell degranulation and IFN-γ secretion engaged through suboptimal TCR triggering (30). Those T_{EM} $CD4^+NKG2D^+$ T cells were found in Wegener

Figure 5. $CD4^+NKG2D^+$ T cells are increased posttherapy in patients experiencing prolonged OS. Total lymphocyte counts (A), proportions of $CD4^+NKG2D^+$ (B), or $CD8^+$ $NKG2D^+$ (C) T cells at C0, C1, and C2 were analyzed according to a stratification of patients based on their OS (<227 or >227 days, the median survival of the whole cohort). D, proportions of $CD4^+$ $NKG2D^+$ T cells after several treatment cycles in 18 patients with metastatic melanoma treated with conventional therapies (including DTIC, fotemustine, isolated limb perfusion, and vaccines) stratified by their OS (<385 or >385 days, the median survival of this cohort). The frequency variations during treatment were analyzed using the paired Student t test and subgroup comparisons were analyzed by the Student t test. (*, $P < 0.05$; **, $P < 0.01$; ***, $P < 0.001$; ns, not significant).
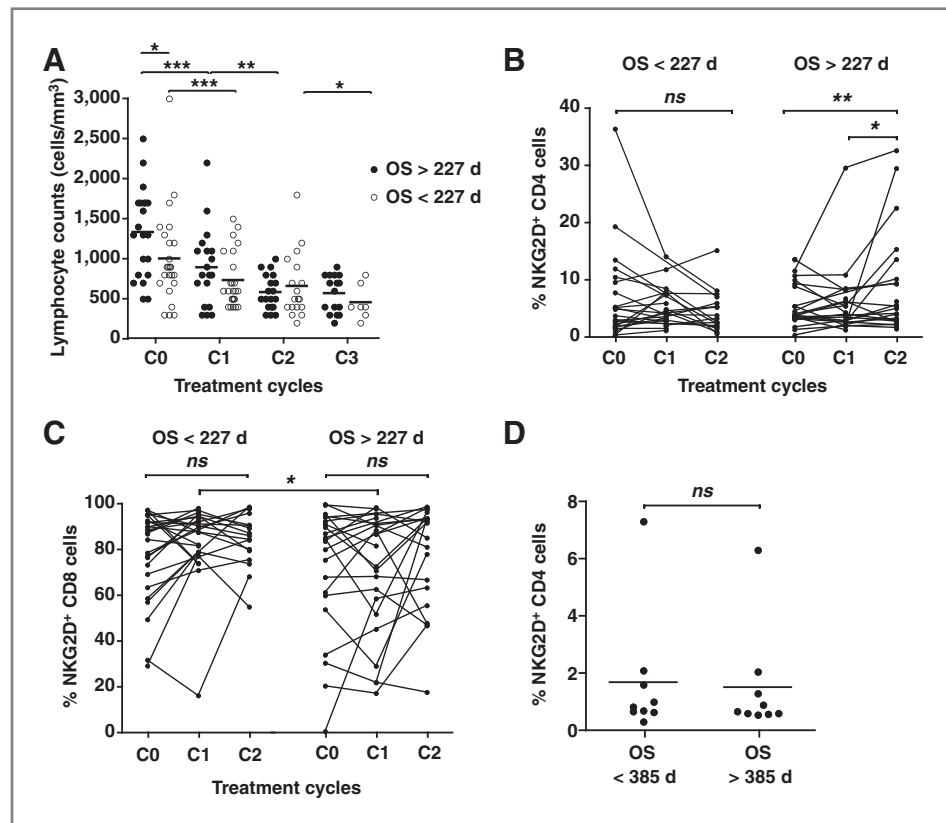
granulomata in close association with MIC[+] and IL-15^{+} cells and CD208 dendritic cells (37). It is known that IL-15 upregulates NKG2D expression on T cells and MIC expression on inflamed tissues and drives T_{EM} differentiation and proliferation, culminating in exacerbation of autoimmune diseases (39, 41). Meresse and colleagues elegantly demonstrated in CD8^{+} T cells that dysregulated IL-15 expression promotes the NKG2D/DAP10 signaling pathway leading to CTL cytotoxic activity independently of the engagement of the TCR, transforming CTL into "LAK-like"LAK-like cells (31). As for CD8^{+} T cells, lamina propria CD4^{+} T cells from Crohn's disease expressing NKG2D, Th1 cytokines, and perforin were functionally active through MICA/NKG2D interactions (40). Third, an increased frequency of double-positive CD4^{+}CD8^{+}αβ T cells (DP cells) was reported in Hodgkin lymphoma, human breast cancer pleural effusions (29), and in melanoma (42). However, these DP cells express high levels of CD8αβ, low levels of CD4, and produce Th2 cytokines upon HLA class I–restricted recognition of tumor cells and normal cells, suggesting that they are "regulatory" CD8^{+} T cells specific for self-antigens. Fourth, Maccalli and colleagues characterized CD4^{−} and CD8 T-cell clones from melanoma lesions for their dependency on TCR versus NKG2D in the recognition patterns of melanoma cells. Very few T-cell clones were CD4^{+} NKG2D^{+} and they recognized tumor cells mainly in a MHC class II–dependent fashion. Moreover, MICA/B expression was rather low in lymph node melanoma, whereas ULBP-2 was more prominent and functionally relevant (33). In our report, CD4^{+}NKG2D^{+} T cells shared biologic and functional features with proinflammatory CD4^{+}NKG2D^{+} T cells. Indeed, the CD4^{+}NKG2D^{+} T-cell subset that we observed in these patients with metastatic melanoma were enriched with T_{EM} cells, expressed low levels of CD8αβ and high levels of CD4, secreted Th1 cytokines, and could proliferate upon suboptimal TCR triggering along with NKG2D and/or CD122 engagement. The major difference is the lack of NK cell receptor expression. Only NKG2D and CD161 (29, 41–44) were expressed in this cohort CD4+NKG2D^{+} T cells.

The proof-of-principle that CD4^{+} T cells can be therapeutically harnessed against metastatic melanoma has been brought up by Hunder and colleagues, where they used IL-2 and IL-7 to differentiate tumor-specific CD4^{+} T cells (43). Others have found that naïve CD4^{+} T cells after adoptive T-cell transfer can be cytotoxic and highly contribute to tumor rejection (45). Such efficient T-cell response strongly relied upon lymphopenia and common γ chain (such as IL-15). Furthermore, an appropriate dendritic cell or monocyte/CD4^{+} T-cell cross-talk will lead to both IL-15–driven IL-12 production by dendritic cell, and enhanced proliferation and polarization of Th1 cells (46). Cytokine/antibody immune complexes to IL-15 or IL-2 or IL-7 may mimic the effects of lymphopenia required for such an efficient triggering of naïve CD4^{+} T cells. Therefore, it is likely that the combination of temozolomide and sorafenib, through prolonged lymphopenia, may foster an environment for the proper polarization and expansion of effector CD4^{+} T cells in a tumor milieu providing the right costimulatory molecules (IL-15Rα and MICA/B). Supporting this premise, our transcriptional profiling indicates that the IL-15/IL-15Rα signaling pathway and Th1 signatures are induced in lesions posttherapy (Supplementary Fig. S6).

In the absence of IL-15Rα induction, however, many strategies could be envisaged to compensate these patients. Cis- or trans-stimulating IL-2Rβγ through stabilized IL-15–based approaches have been tested in preclinical models (47). Indeed, IL-15/IL-15Rα-Fc, IL-15/IL-15Rα fusion proteins, IL-15 fused to the human antibody fragment (scFv) specific of a tumor antigen or the tumor stromal fibroblast activation protein, IL-15 gene therapy (such as the hydrodynamic injection of plasmids encoding IL-15 or IL-15 engineered oncolytic viruses) have all been reported to be efficient against mouse tumors.

Our data suggest that a subset of CD4^{+} T cells (expressing NKG2D) becomes biologically significant in that they may be engaged by IL-15Rα and MICA/B expressed on tumor cells and/or monocytes (either through sorafenib or spontaneously, respectively) to secrete high levels of Th1 cytokines. We cannot exclude that other NKG2D^{+}-expressing effectors could be implicated as we could also monitor CD8^{+} T cells infiltrating tumors. However, it seems that only CD4^{+}NKG2D^{+} T cells could be augmented after two cycles of therapy, which turned out to be clinically relevant and associated with longer OS.

In conclusion, our data suggest that CD4^{+}NKG2D^{+} T cells could be tuned functionally by induction of IL-15Rα. This observation could have some clinical impact, as compounds inducing or mimicking IL-15 transpresentation are currently under development for the treatment of cancer.

Disclosure of Potential Conflicts of Interest

C. Robert is a consultant/advisory board member of Roche, GlaxoSmithKline, Bristol-Myers Squibb, Merck, and Novartis. No potential conflicts of interest were disclosed by the other authors.

Authors' Contributions

Conception and design: A.I. Romero, N. Chaput, C. Robert, L. Zitvogel
Development of methodology: A.I. Romero, V. Poirier-Colame, S. Rusakiewicz, P. Vielh, C. Robert, L. Zitvogel
Acquisition of data (provided animals, acquired and managed patients, provided facilities, etc.): A.I. Romero, V. Poirier-Colame, S. Rusakiewicz, N. Jacquelot, K. Chaba, E. Mortier, S. Caillat-Zucman, C. Flament, M. Messaoudene, P. Vielh, P. Dessen, C. Porta, C. Mateus, M. Ayyoub, D. Valmori, C. Robert
Analysis and interpretation of data (e.g., statistical analysis, biostatistics, computational analysis): A.I. Romero, N. Chaput, S. Rusakiewicz, N. Jacquelot, C. Flament, A. Aupérin, M. Ayyoub, D. Valmori, L. Zitvogel
Writing, review, and/or revision of the manuscript: A.I. Romero, N. Chaput, S. Rusakiewicz, S. Caillat-Zucman, A. Caignard, M. Messaoudene, P. Dessen, C. Porta, A. Eggermont, C. Robert, L. Zitvogel
Administrative, technical, or material support (i.e., reporting or organizing data, constructing databases): V. Poirier-Colame, P. Vielh, L. Zitvogel
Study supervision: N. Chaput, Y. Jacques, C. Robert, L. Zitvogel

Acknowledgments

Grant Support

References

1. Tawbi HA, Kirkwood JM. Management of metastatic melanoma. Semin Oncol 2007;34:532–45.
2. Lee ML, Tomsu K, Von Eschen KB. Duration of survival for disseminated malignant melanoma: results of a meta-analysis. Melanoma Res 2000;10:81–92.
3. Agarwala SS, Kirkwood JM, Gore M, Dreno B, Thatcher N, Czarnetski B, et al. Temozolomide for the treatment of brain metastases associated with metastatic melanoma: a phase II study. J Clin Oncol 2004; 22:2101–7.
4. Middleton MR, Grob JJ, Aaronson N, Fierlbeck G, Tilgen W, Seiter S, et al. Randomized phase III study of temozolomide versus dacarbazine in the treatment of patients with advanced metastatic malignant melanoma. J Clin Oncol 2000;18:158–66.
5. Davies H, Bignell GR, Cox C, Stephens P, Edkins S, Clegg S, et al. Mutations of the BRAF gene in human cancer. Nature 2002;417: 949–54.
6. Eisen T, Ahmad T, Flaherty KT, Gore M, Kaye S, Marais R, et al. Sorafenib in advanced melanoma: a phase II randomised discontinuation trial analysis. Br J Cancer 2006;95:581–6.
7. Flaherty KT, Lee SJ, Zhao F, Schuchter LM, Flaherty L, Kefford R, et al. Phase III trial of carboplatin and paclitaxel with or without sorafenib in metastatic melanoma. J Clin Oncol 2013;31:373–9.
8. Hauschild A, Agarwala SS, Trefzer U, Hogg D, Robert C, Hersey P, et al. Results of a phase III, randomized, placebo-controlled study of sorafenib in combination with carboplatin and paclitaxel as second-line treatment in patients with unresectable stage III or stage IV melanoma. J Clin Oncol 2009;27:2823–30.
9. Amaravadi RK, Schuchter LM, McDermott DF, Kramer A, Giles L, Gramlich K, et al. Phase II trial of temozolomide and sorafenib in advanced melanoma patients with or without brain metastases. Clin Cancer Res 2009;15:7711–8.
10. Hodi FS, O'Day SJ, McDermott DF, Weber RW, Sosman JA, Haanen JB, et al. Improved survival with ipilimumab in patients with metastatic melanoma. N Engl J Med 2010;363:711–23.
11. Robert C, Thomas L, Bondarenko I, O'Day S, Weber J, Garbe C, et al. Ipilimumab plus dacarbazine for previously untreated metastatic melanoma. N Engl J Med 2011;364:2517–26.
12. Boon T, Coulie PG, Van den Eynde BJ, van der Bruggen P. Human T cell responses against melanoma. Annu Rev Immunol 2006;24: 175–208.
13. Arlen PM, Gulley JL, Parker C, Skarupa L, Pazdur M, Panicali D, et al. A randomized phase II study of concurrent docetaxel plus vaccine versus vaccine alone in metastatic androgen-independent prostate cancer. Clin Cancer Res 2006;12:1260–9.
14. Schlom J, Arlen PM, Gulley JL. Cancer vaccines: moving beyond current paradigms. Clin Cancer Res 2007;13:3776–82.
15. Zitvogel L, Apetoh L, Ghiringhelli F, Andre F, Tesniere A, Kroemer G. The anticancer immune response: indispensable for therapeutic success? J Clin Invest 2008;118:1991–2001.
16. Ghiringhelli F, Apetoh L, Tesniere A, Aymeric L, Ma Y, Ortiz C, et al. Activation of the NLRP3 inflammasome in dendritic cells induces IL-1beta–dependent adaptive immunity against tumors. Nat Med 2009; 15:1170–8.
17. Ramakrishnan R, Assudani D, Nagaraj S, Hunter T, Cho HI, Antonia S, et al. Chemotherapy enhances tumor cell susceptibility to CTL-mediated killing during cancer immunotherapy in mice. J Clin Invest 2010; 120:1111–24.
18. Ladoire S, Arnould L, Apetoh L, Coudert B, Martin F, Chauffert B, et al. Pathologic complete response to neoadjuvant chemotherapy of breast carcinoma is associated with the disappearance of tumor-infiltrating foxp3+ regulatory T cells. Clin Cancer Res 2008;14:2413–20.
19. Vincent J, Mignot G, Chalmin F, Ladoire S, Bruchard M, Chevriaux A, et al. 5-Fluorouracil selectively kills tumor-associated myeloid-derived suppressor cells resulting in enhanced T cell-dependent antitumor immunity. Cancer Res 2010;70:3052–61.
20. Chapon M, Randriamampita C, Maubec E, Badoual C, Fouquet S, Wang SF, et al. Progressive upregulation of PD-1 in primary and metastatic melanomas associated with blunted TCR signaling in infiltrating T lymphocytes. J Invest Dermatol 2011;131:1300–7.
21. Koebel CM, Vermi W, Swann JB, Zerafa N, Rodig SJ, Old LJ, et al. Adaptive immunity maintains occult cancer in an equilibrium state. Nature 2007;450:903–7.
22. Zitvogel L, Mayordomo JI, Tjandrawan T, DeLeo AB, Clarke MR, Lotze MT, et al. Therapy of murine tumors with tumor peptide-pulsed dendritic cells: dependence on T cells, B7 costimulation, and T helper cell 1–associated cytokines. J Exp Med 1996;183:87–97.
23. Vetter CS, Lieb W, Brocker EB, Becker JC. Loss of nonclassical MHC molecules MIC-A/B expression during progression of uveal melanoma. Br J Cancer 2004;91:1495–9.
24. Diefenbach A, Jensen ER, Jamieson AM, Raulet DH. Rae1 and H60 ligands of the NKG2D receptor stimulate tumour immunity. Nature 2001;413:165–71.
25. Smyth MJ, Swann J, Cretney E, Zerafa N, Yokoyama WM, Hayakawa Y. NKG2D function protects the host from tumor initiation. J Exp Med 2005;202:583–8.
26. Kruit WH, van Ojik HH, Brichard VG, Escudier B, Dorval T, Dreno B, et al. Phase 1/2 study of subcutaneous and intradermal immunization with a recombinant MAGE-3 protein in patients with detectable metastatic melanoma. Int J Cancer 2005;117:596–604.
27. Valmori D, Souleimanian NE, Tosello V, Bhardwaj N, Adams S, O'Neill D, et al. Vaccination with NY-ESO-1 protein and CpG in Montanide induces integrated antibody/Th1 responses and CD8 T cells through cross-priming. Proc Natl Acad Sci U S A 2007;104:8947–52.
28. Livak KJ, Schmittgen TD. Analysis of relative gene expression data using real-time quantitative PCR and the 2(−delta delta C(T)) method. Methods 2001;25:402–8.
29. Desfrancois J, Derre L, Corvaisier M, Le Mevel B, Catros V, Jotereau F, et al. Increased frequency of nonconventional double positive CD4CD8 alphabeta T cells in human breast pleural effusions. Int J Cancer 2009;125:374–80.
30. Fasth AE, Bjorkstrom NK, Anthoni M, Malmberg KJ, Malmstrom V. Activating NK-cell receptors co-stimulate CD4(+)CD28(−) T cells in patients with rheumatoid arthritis. Eur J Immunol 2010;40: 378–87.
31. Meresse B, Chen Z, Ciszewski C, Tretiakova M, Bhagat G, Krausz TN, et al. Coordinated induction by IL15 of a TCR-independent NKG2D signaling pathway converts CTL into lymphokine-activated killer cells in celiac disease. Immunity 2004;21:357–66.
32. Stehle F, Schulz K, Fahldieck C, Kalich J, Lichtenfels R, Riemann D, et al. Reduced immunosuppressive properties of axitinib in comparison with other tyrosine kinase inhibitors. J Biol Chem 2013;288: 16334–47.
33. Maccalli C, Nonaka D, Piris A, Pende D, Rivoltini L, Castelli C, et al. NKG2D-mediated antitumor activity by tumor-infiltrating lymphocytes and antigen-specific T-cell clones isolated from melanoma patients. Clin Cancer Res 2007;13:7459–68.
34. Groh V, Smythe K, Dai Z, Spies T. Fas-ligand-mediated paracrine T cell regulation by the receptor NKG2D in tumor immunity. Nat Immunol 2006;7:755–62.
35. Groh V, Wu J, Yee C, Spies T. Tumour-derived soluble MIC ligands impair expression of NKG2D and T-cell activation. Nature 2002; 419:734–8.
36. Dai Z, Turtle CJ, Booth GC, Riddell SR, Gooley TA, Stevens AM, et al. Normally occurring NKG2D+CD4+ T cells are immunosuppressive and inversely correlated with disease activity in juvenile-onset lupus. J Exp Med 2009;206:793–805.

37. Capraru D, Muller A, Csernok E, Gross WL, Holl-Ulrich K, Northfield J, et al. Expansion of circulating NKG2D+ effector memory T-cells and expression of NKG2D-ligand MIC in granulomaous lesions in Wegener's granulomatosis. Clin Immunol 2008;127:144–50.

38. Komocsi A, Lamprecht P, Csernok E, Mueller A, Holl-Ulrich K, Seitzer U, et al. Peripheral blood and granuloma CD4(+)CD28(−) T cells are a major source of interferon-gamma and tumor necrosis factor-alpha in Wegener's granulomatosis. Am J Pathol 2002;160:1717–24.

39. Groh V, Bruhl A, El-Gabalawy H, Nelson JL, Spies T. Stimulation of T cell autoreactivity by anomalous expression of NKG2D and its MIC ligands in rheumatoid arthritis. Proc Natl Acad Sci U S A 2003; 100:9452–7.

40. Allez M, Tieng V, Nakazawa A, Treton X, Pacault V, Dulphy N, et al. CD4+NKG2D+ T cells in Crohn's disease mediate inflammatory and cytotoxic responses through MICA interactions. Gastroenterology 2007;132:2346–58.

41. Roberts AI, Lee L, Schwarz E, Groh V, Spies T, Ebert EC, et al. NKG2D receptors induced by IL-15 costimulate CD28-negative effector CTL in the tissue microenvironment. J Immunol 2001;167:5527–30.

42. Desfrancois J, Moreau-Aubry A, Vignard V, Godet Y, Khammari A, Dreno B, et al. Double positive CD4CD8 alphabeta T cells: a new tumor-reactive population in human melanomas. PLoS ONE 2010;5: e8437.

43. Hunder NN, Wallen H, Cao J, Hendricks DW, Reilly JZ, Rodmyre R, et al. Treatment of metastatic melanoma with autologous CD4+ T cells against NY-ESO-1. N Engl J Med 2008;358:2698–703.

44. Biswas SK, Mantovani A. Macrophage plasticity and interaction with lymphocyte subsets: cancer as a paradigm. Nat Immunol 2010;11: 889–96.

45. Xie Y, Akpinarli A, Maris C, Hipkiss EL, Lane M, Kwon EK, et al. Naive tumor-specific CD4(+) T cells differentiated in vivo eradicate established melanoma. J Exp Med 2010;207:651–67.

46. Ohteki T, Suzue K, Maki C, Ota T, Koyasu S. Critical role of IL-15–IL-15R for antigen-presenting cell functions in the innate immune response. Nat Immunol 2001;2:1138–43.

47. Ochoa MC, Mazzolini G, Hervas-Stubbs S, de Sanmamed MF, Berraondo P, Melero I. Interleukin-15 in gene therapy of cancer. Curr Gene Ther 2013;13:15–30.

Cancer Research

AACR American Association for Cancer Research

Regulation of CD4$^+$NKG2D$^+$ Th1 Cells in Patients with Metastatic Melanoma Treated with Sorafenib: Role of IL-15R α and NKG2D Triggering

Ana I. Romero, Nathalie Chaput, Vichnou Poirier-Colame, et al.

Updated version	Access the most recent version of this article at: doi:10.1158/0008-5472.CAN-13-1186
Supplementary Material	Access the most recent supplemental material at: http://cancerres.aacrjournals.org/content/suppl/2013/11/06/0008-5472.CAN-13-1186.DC1

Cited articles	This article cites 47 articles, 18 of which you can access for free at: http://cancerres.aacrjournals.org/content/74/1/68.full#ref-list-1
Citing articles	This article has been cited by 1 HighWire-hosted articles. Access the articles at: http://cancerres.aacrjournals.org/content/74/1/68.full#related-urls

E-mail alerts	Sign up to receive free email-alerts related to this article or journal.
Reprints and Subscriptions	To order reprints of this article or to subscribe to the journal, contact the AACR Publications Department at pubs@aacr.org.
Permissions	To request permission to re-use all or part of this article, use this link http://cancerres.aacrjournals.org/content/74/1/68. Click on "Request Permissions" which will take you to the Copyright Clearance Center's (CCC) Rightslink site.